Organometallics **2001,** *20,* 713−720

Theoretical Study on the Structure and Electronic Properties of Mono- and Bimetallic Methylzinc Complexes Containing Bidentate Ligands

Jennie Weston[†]

Institut für Organische Chemie und Makromolekulare Chemie der
Friedrich-Schiller-Universität, Humboldtstrasse 10, D-07443 Jena, Germany

Received September 12, 2000

The reactions of 1 and 2 equiv of dimethylzinc with 10 different model ligands, each containing two heteroatoms, were investigated at the HF and B3LYP level of theory. As the heteroatom combination is varied, the stability of the **A**·ZnMe (formed from acidic ligands) and **B**·$ZnMe_2$ (formed from nonacidic ligands) species will decrease as follows: **A**-type ligands, NS > SS > NO > NN> OO; **B**-type ligands, NN > NO > NS > OO > SS. Formation of the **A**·ZnMe complex is exothermic by ca. −20 kcal/mol when the ligand contains N and/or O and ca. −30 kcal/mol when S is present. ΔE_f is a magnitude of order larger (−2 to −9 kcal/mol) for the formation of **B**·$ZnMe_2$ complexes. Only monometallic **A**·ZnMe species are capable of complexing with a second equivalent of dimethylzinc to form a bimetallic **A**·Zn_2Me_3 species. NBO analyses provide no indication for a bonding Zn−Zn interaction. The 3d orbitals on zinc are not involved in bonding or hyperconjugative interactions in either the mono- or the bimetallic organozinc species. Zinc−carbon and zinc−ligand bonds to O, N, and S have a nearly pure s character at zinc.

Introduction

Aromatic and aliphatic aldehydes can be effectively enantioselectively alkylated by dialkylzinc compounds to give chiral alcohols in excellent yields and extremely high enantiomeric purities (often >95% ee).[1,2,3] In order for this reaction to take place, a catalytic amount of a chiral bidentate chelating agent such as the widely employed (−)-3-*exo*-(dimethylamino)isoborneol ((−)-DAIB)[4] must be present (Figure 1).[5,6] Deprotonation of the chelating agent by the alkylzinc compound accompanied by the evolution of an unreactive hydrocarbon (RH) results in the catalyst precursor **1**. Extensive mechanistic studies of both experimental[7−9] and theoretical nature[10,11] succeeded in showing that the monomeric precursor **1** (active form) lies in equilibrium with its (inactive) dimeric form **2**.[7] The dimer **2** acts as a chiral reservoir, which gives rise to a very interesting nonlinear[12] effect.[8,9]

A general characteristic of this reaction is that 2 equiv of the dialkylzinc compound is necessary. The catalytic cycle can be started by adding a second equivalent of the dialkylzinc compound, which breaks up the dimer **2** to form an intermediate bimetallic zinc species **3**, which then complexes with the aldehyde. Alternatively, the aldehyde can be added *before* the second equivalent of the organozinc reagent. Both pathways result in the formation of the intermediate species **5**. The alkyl anion transfer occurs in **5** and has been shown to be the rate-determining step of the reaction.[9]

Most of the successful results reported in the literature employ a β-amino alcohol as the chiral ligand.[13] β-Amino thiols have also been shown to catalyze the

---

[†] Fax: +49 (0) 3641-9-48212. E-mail: Jennie.Weston@rz.uni-jena.de.

(1) Noyori, R. *Asymmetric Catalysis in Organic Synthesis*; Wiley: New York, 1994. Knochel, P.; Singer, R. D. *Chem. Rev.* **1993**, *93*, 2117. Knochel, P. In *Comprehensive Organic Synthesis*; Trost, B. M., Ed.; Pergamon Press: Oxford, U.K., 1991. Noyori, R.; Kitamura, M. In *Modern Synthetic Methods*; Scheffold, R., Ed.; Springer-Verlag: Berlin, 1989. Oguni, N.; Omi, T. *Tetrahedron Lett.* **1984**, *25*, 2823. Mukaiyama, T.; Soai, K.; Sato, T.; Shimizu, H.; Suzuki, K. *J. Am. Chem. Soc.* **1979**, *101*, 1455.

(2) Noyori, R.; Kitamura, M. *Angew. Chem.* **1991**, *103*, 34; *Angew. Chem., Int. Ed. Engl.* **1991**, *30*, 49.

(3) Soai, K.; Niwa, S. *Chem. Rev.* **1992**, *92*, 833.

(4) Chittenden, R. A.; Cooper, G. H. *J. Chem. Soc. C* **1970**, 49.

(5) Kitamura, M.; Suga, S.; Kawai, K.; Noyori, R. *J. Am. Chem. Soc.* **1986**, *108*, 6071. Boersma, J. In *Comprehensive Organometallic Chemistry*; Wilkinson, G., Stone, F. G. A., Abel, E. W., Eds.; Pergamon Press: Oxford, U.K., 1982; Vol. 2.

(6) Noyori, R.; Suga, S.; Kawai, K.; Okada, S.; Kitamura, M.; Oguni, N.; Hayashi, M.; Kaneko, T.; Matsuda, Y. *J. Organomet. Chem.* **1990**, *382*, 19.

(7) Kitamura, M.; Yamakawa, M.; Oka, H.; Suga, S.; Noyori, R. *Chem. Eur. J.* **1996**, *2*, 1173. Kitamura. M.; Suga, S.; Niwa, M.; Noyori, R.; Zhai, Z. X.; Suga, H. *J. Phys. Chem.* **1994**, *98*, 12776.

(8) Kitamura, M.; Suga, S.; Oka, H.; Noyori, R. *J. Am. Chem. Soc.* **1998**, *120*, 9800. Kitamura, M.; Suga, S.; Niwa, M.; Noyori, R. *J. Am. Chem. Soc.* **1995**, *117*, 4832. Oguni, N.; Matsuda, Y.; Kaneko, T. *J. Am. Chem. Soc.* **1998**, *110*, 7877.

(9) Kitamura, M.; Okada, S.; Suga, S.; Noyori, R. *J. Am. Chem. Soc.* **1989**, *111*, 4028.

(10) Yamakawa, M.; Noyori, R. *Organometallics* **1999**, *18*, 128. Yamakawa, M.; Noyori, R. *J. Am. Chem. Soc.* **1995**, *117*, 6327.

(11) Goldfuss, B.; Houk, K. N. *J. Org. Chem.* **1998**, *63*, 8998. Vidal-Ferran, A.; Moyano, A.; Pericàs, M. A.; Riera, A. *Tetrahedron Lett.* **1997**, *38*, 8773.

(12) Girard, C.; Kagan, H. B. *Angew. Chem.* **1998**, *110*, 3089; *Angew. Chem., Int. Ed. Engl.* **1998**, *37*, 2922. Blackmond, D. G. *J. Am. Chem. Soc.* **1997**, *119*, 12934 and literature contained therein.

(13) See for example: Paleo, M. R.; Cabeza, I.; Sardina, J. *J. Org. Chem.* **2000**, *65*, 2108. Palmieri, G. *Eur. J. Org. Chem.* **1999**, 805. Cho, B. T.; Chun, Y. S. *Tetrahedron: Asymmetry* **1998**, *9*, 1489. Bringmann, G.; Breuning, M. *Tetrahedron: Asymmetry* **1998**, *9*, 667. Shi, M.; Satoh, Y.; Masaki, Y. *J. Chem. Soc., Perkin Trans. 1* **1998**, 2547. Shibata, T.; Tabira, H.; Soai, K. *J. Chem. Soc., Perkin Trans. 1* **1998**, 177. Bolm, C.; Schlingloff, G.; Harms, K.; *Chem. Ber.* **1992**, *125*, 1191. Corey, E. J.; Yuen, P. W.; Hannon, F. J.; Wierda, D. A. *J. Org. Chem.* **1990**, *55*, 784 and literature contained therein.

10.1021/om000783x CCC: $20.00
Publication on Web 01/18/2001

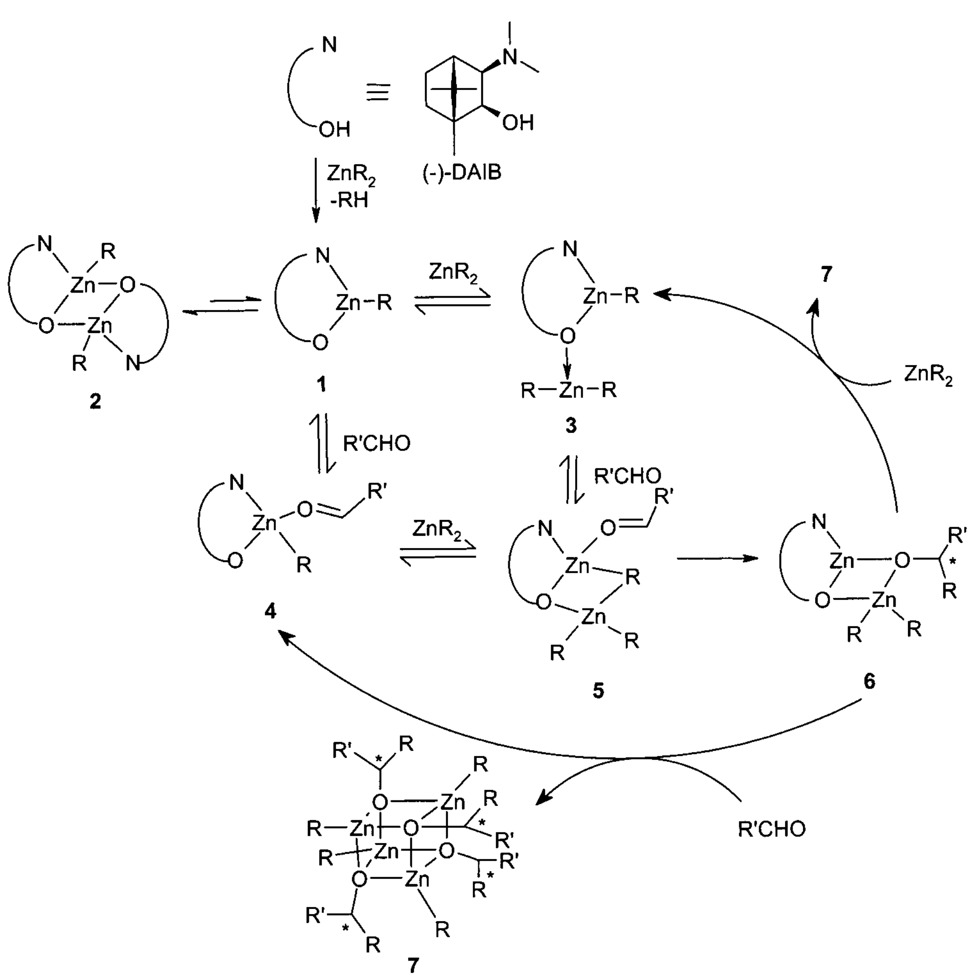

Figure 1. Catalytic cycle postulated by Noyori et al.[7−10] for the (−)-DAIB-promoted enantioselective alkylation of aldehydes by dialkylzinc compounds.

addition of diethylzinc to benzaldehyde in high enantiomeric excess.[14,15] Chiral dialkyldiamines and diether compounds are much less satisfactory as ligands. TMEDA, a successful ligand in other areas of organometallic chemistry, performs sluggishly and barely manages to catalyze the addition of diethylzinc to benzaldehyde. Addition of 0.02 equiv of TMEDA results in a chemical yield of only 10% yield after 1 h.[2] 1,2-Dimethoxyethane does not catalyze the addition at all.[2] The few cases reported in the literature where a diamine or a OO-chelate ligand functions effectively as a catalyst occurs when the ligand contains a NH or OH group that can be deprotonated.[16,17]

As mentioned above, extensive experimental and computational studies have led to a detailed understanding of the mechanism of the β-amino alcohol catalyzed reaction. In addition, the nature of the Zn−C bond in dimethyl- and diphenylzinc has been analyzed in depth at the CCSD(T) level of theory.[18] When one moves away either from simple dialkyl-/diarylzinc compounds or from the β-amino alcohol catalyzed case, not much is known about the structure and electronic properties of the mono- and bimetallic zinc species generated when a dialkylzinc compound reacts with a bidentate ligand containing two heteroatoms. X-ray structures of the bimetallic intermediates generated show that these compounds prefer a dimeric structure in the solid state,[9,15,19] whereas Noyori could clearly show that the monometallic species is responsible for the catalytic activity. Lack of information about the monometallic catalyst precursor prompted the present

---

[14] See for example: Chelucci, G.; Berta, D.; Fabbri, D.; Pinna, G. A.; Saba, A.; Ulgheri, F. *Tetrahedron: Asymmetry* **1998**, *9*, 1933. Kossenjans, M.; Martens, J. *Tetrahedron: Asymmetry* **1998**, *9*, 1409. Anderson, J. C.; Harding, M. *Chem. Commun.* **1998**, 393. Kellogg, R. M.; Hof, R. P. *J. Chem. Soc., Perkin Trans. 1* **1996**, 1651. Gibson, C. L. *J. Chem. Soc., Chem. Commun.* **1996**, 645. Kang, J.; Lee, J. W.; Kim. J. I. *Tetrahedron Lett.* **1995**, *36*, 4265. Masaki, Y.; Satoh, Y.; Makihara, T.; Shi, M. *Chem. Pharm. Bull.* **1996**, *44*, 454 and literature contained therein.

[15] Nakano, H.; Kumagai, N.; Matsuzaki, H.; Kabuto, C.; Hongo, H. *Tetrahedron: Asymmetry* **1997**, *8*, 1391. Rijnberg, E.; Hovestad, N. J.; Kleij, A. W.; Jastrzebski, J. T. B. H.; Boersma, J.; Janssen, M. D.; Spek, A. L.; van Koten, G. *Organometallics* **1997**, *16*, 2847.

[16] Asami, M.; Inoue, S. *Bull. Chem. Soc. Jpn.* **1997**, *70*, 1687. Eilers, J.; Wilken, J.; Martens, J. *Tetrahedron: Asymmetry* **1996**, *7*, 2343. Dai, W. M.; Zhu, H. J.; Hao, X. J. *Tetrahedron: Asymmetry* **1996**, *7*, 1245. Pini, D.; Mastantuono, A.; Uccello-Barretta, G.; Iuliano, A.; Salvadori, P.; *Tetrahedron* **1993**, *49*, 9613. Rosini, C.; Franzini, L.; Iuliano, A.; Pini, D.; Salvadori, P. *Tetrahedron: Asymmetry* **1991**, *2*, 363. Niwa, S.; Soai, K. *J. Chem. Soc., Perkin Trans. 1* **1991**, 2717.

[17] Ding, K.; Ishii, A.; Mikami, K. *Angew. Chem.* **1999**, *111*, 519; *Angew. Chem., Int. Ed.* **1999**, *38*, 387. Rheiner, P. B.; Sellner, H.; Seebach, D. *Helv. Chim. Acta* **1997**, *80*, 2027. Hu, Q. S.; Huang, W. S.; Vitharana, D.; Zhang, X. F.; Pu, L. *J. Am. Chem. Soc.* **1997**, *119*, 12454. Huang, W. S.; Hu, Q. S.; Pu, L. *J. Org. Chem.* **1998**, *63*, 2798. Huang, W. S.; Hu, Q. S.; Pu, L. *J. Org. Chem.* **1998**, *63*, 1364. Prasad, K. R. K.; Joshi, N. N. *Tetrahedron: Asymmetry* **1996**, *7*, 1957. Rosini, C.; Franzini, L.; Pini, D.; Salvadori, P. *Tetrahedron: Asymmetry* **1990**, *1*, 587.

[18] Antes, I.; Frenking, G. *Organometallics* **1995**, *14*, 4263.

[19] Goldfuss, B.; Steigelmann, M.; Rominger, F. *Eur. J. Org. Chem.* **2000**, 1785. Goldfuss, B.; Kahn, S. I.; Houk, K. N. *Organometallics* **1999**, *18*, 2927.

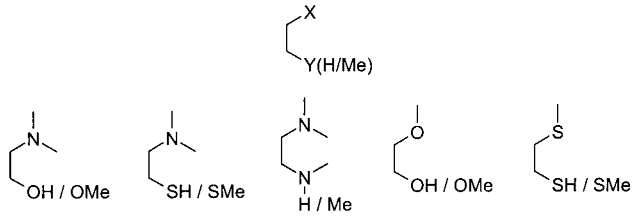

8a / 8b **9a / 9b** **10a / 10b** **11a / 11b** **12a / 12b**

Figure 2. Set of 10 model ligands selected for study. **A**-type ligands contain a YH group and **B**-type ligands a nonacidic YMe unit.

study, which is essentially a ligand screening study performed at the HF and B3LYP level of theory on a series of 10 model ligands (Figure 2), one of which (ligand **8a**) has previously been computationally investigated by Noyori et al.[10] The goal of this study is to show how variation of the heteroatom in the bidentate ligand affects the structure and energetics of the mono- and bimetallic species generated upon reaction with a dialkylzinc compound (dimethylzinc in this study). In addition, the effect of the ligand on both the Zn−C bond(s) present and on the Lewis acidity of the Zn center(s) is investigated in detail. These findings should contribute to the further understanding of the general reaction mechanism(s) of biomimetric, bifunctional zinc catalysts, which work as a template to bring a carbonyl compound together with a alkyl anion in such a manner that the alkyl group can be efficiently and effectively transferred to the carbonyl C═O bond.

Computational Details

Full conformational searches using the program SPARTAN[20] were performed for all species of interest using the semiempirical methods MNDO/d,[21] AM1,[22] and PM3.[23] All three methods were employed, since a recent investigation[24] has shown that none of the three methods can be relied upon to correctly predict the overall structure of organozinc compounds—especially when multiple zinc−heteroatom bonds are present. PM3, for example, fails to describe Zn−O interactions correctly but is the best method for Zn−N bonds.[24] MNDO(d) has difficulties with Zn−S interactions but correctly describes many bioorganic complexes.[24] AM1 behaves similarly to PM3; the average errors found, however, are ca. 30% larger than for PM3.[24]

The semiempirical structures then served as starting geometries for optimizations at the HF/6-311+G(d,p) level of theory. The HF structures were then subjected to reoptimization at the B3LYP/6-311+G(d,p) level and, for compound **8a**·ZnMe, at the MP2/6-311+G(d,p) level. All ab initio calculations were performed using the Gaussian 98[25] suite of programs. All stationary points found were characterized as energy minima by calculating their vibrational frequencies. The relative stabilities and energies of formation reported in this article contain a correction for the zero-point vibrational energy (a scaling factor of 0.91 was employed for the HF results;[26] the B3LYP results were not scaled). Atomic charges and hyperconjugative interaction energies were obtained using the natural bond orbital (NBO) analysis of Reed et al.[27] as implemented in Gaussian98.

It proved absolutely necessary to use the large 6-311+G(d,p) basis set in this study. Enthalpies of reaction calculated for the monometallic zinc compounds on the HF level of theory with the smaller 6-311G basis were calculated to be ca. 10 kcal too negative due to basis set superposition errors (BSSE[28]). An estimation of the BSSE encountered for the 6-311+G(d,p) basis using the counterpoise correction procedure[29] showed that, in contrast to the smaller basis set, the error is approximately 1−2 kcal/mol and can be neglected. For the B3LYP method, massive convergence problems (especially for the bimetallic species) in addition to a significant BSSE occurred at the B3LYP/6-311G level, both of which could be eliminated only upon employment of the larger 6-311+G(d,p) basis set.

Recent B3LYP calculations on monometallic zinc species have demonstrated that the 6-311++G(d,p) basis set is capable of reproducing experimental ΔG values for the addition/loss of ligand molecules to within 1−2 kcal/mol.[30] Calculation of the enthalpy of formation for **8a**·ZnMe using the larger 6-311++G(d,p) basis yielded practically the same value (−22.3 kcal/mol) as for the 6-311+G(d,p) basis (−22.7), thus demonstrating that the B3LYP method is already self-consistent for the smaller basis used in this study.

To reduce the number of different conformers that had to be considered, only the syn form of the ligand (necessary for bidentate coordination to zinc) was calculated. The anti form is generally slightly more stable than the syn conformer (1−3 kcal/mol, depending upon the ligand). The equilibria calculated here thus do not include the amount of energy necessary to convert the anti into the syn form. Further relevant computational details are discussed, where necessary, in the following discussion.

Results and Discussion

Five of the ligands considered in this study (**A**H; **8a**−**12a** in Figure 2) contain an acidic proton and are able to react with dialkylzinc compounds (dimethylzinc) to form a monometallic organozinc species (**A**·ZnMe) under generation of an equivalent of hydrocarbon (eq 1). The other five bidentate ligands **B** are nonacidic (compounds **8b**−**12b**) and are capable of complexing with a dialkyl-

---

[20] Spartan is available from Wavefunction, Inc., 19491 von Karman Ave., Suite 370, Irvine, CA.

[21] Thiel, W.; Voityuk, A. A. *J. Phys. Chem.* **1996**, *100*, 616. Thiel, W.; Voityuk, A. A. *Theor. Chim. Acta* **1992**, *81*, 391. Dewar, M. J. S.; Merz, K. M., Jr. *Organometallics* **1986**, *5*, 1494. Dewar, M. J. S.; Thiel, W. *J. Am. Chem. Soc.* **1977**, *99*, 4899.

[22] Dewar, M. J. S.; Merz, K. M., Jr. *Organometallics* **1988**, *7*, 522. Dewar, M. J. S.; Zoebisch, E. G.; Healy, E. F.; Stewart, J. J. P. *J. Am. Chem. Soc.* **1985**, *107*, 3902.

[23] Stewart, J. J. P. *J. Comput. Chem.* **1989**, *10*, 209; 221.

[24] Bräuer, M.; Kunert, M.; Dinjus, E.; Klussmann, M.; Döring, M.; Görls, H.; Anders, E. *J. Mol. Struct. (THEOCHEM)* **2000**, *505*, 289.

[25] Frisch, M. J.; Trucks, G. W.; Schlegel, H. B.; Scuseria, G. E.; Robb, M. A.; Cheeseman, J. R.; Zakrzewski, V. G.; Montgomery, J. A., Jr.; Stratmann, R. E.; Burant, J. C.; Dapprich, S.; Millam, J. M.; Daniels, A. D.; Kudin, K. N.; Strain, M. C.; Farkas, O.; Tomasi, J.; Barone, V.; Cossi, M.; Cammi, R.; Mennucci, B.; Pomelli, C.; Adamo, C.; Clifford, S.; Ochterski, J.; Petersson, G. A.; Ayala, P. Y.; Cui, Q.; Morokuma, K.; Malick, D. K.; Rabuck, A. D.; Raghavachari, K.; Foresman, J. B.; Cioslowski, J.; Ortiz, J. V.; Stefanov, B. B.; Liu, G.; Liashenko, A.; Piskorz, P.; Komaromi, I.; Gomperts, R.; Martin, R. L.; Fox, D. J.; Keith, T.; Al-Laham, M. A.; Peng, C. Y.; Nanayakkara, A.; Gonzalez, C.; Challacombe, M.; Gill, P. M. W.; Johnson, B. G.; Chen, W.; Wong, M. W.; Andres, J. L.; Head-Gordon, M.; Replogle, E. S.; Pople, J. A. *Gaussian 98*, revision A.5; Gaussian, Inc.: Pittsburgh, PA, 1998.

[26] Grev, R. S.; Jansen, C. L.; Schaefer, H. F., III. *J. Chem. Phys.* **1991**, *95*, 5128 and references therein.

[27] Reed, A. E.; Curtiss, L. A.; Weinhold, F. *Chem. Rev.* **1988**, *88*, 899. Reed, A. E.; Weinstock, R. B.; Weinhold, F. J. *J. Chem. Phys.* **1985**, *83*, 735.

[28] Van Duijneveldt, F. B. In *Basis Superposition Error in Molecular Interactions*; Scheiner, S., Ed.; Wiley: New York, 1997. Van Mourik, T.; Wilson, A. K.; Peterson, K. A.; Woon, D. E.; Dunning, T. H., Jr. *Adv. Quantum Chem.* **1999**, *31*, 105.

[29] Van Duijneveldt, F. B.; van Duijneveldt-van de Rijdt, J. G. C. M.; van Lenthe, J. H. *Chem. Rev.* **1994**, *94*, 1873.

[30] Peschke, M.; Blades, A. T.; Kebarle, P. *J. Am. Chem. Soc.* **2000**, *122*, 1492.

Table 1. Enthalpies of Formation (kcal/mol) for the Generation of the Monometallic Organozinc Species 8a·ZnMe−12a·ZnMe and 8b·ZnMe$_2$−12b·ZnMe$_2$

	HF[a]	B3LYP[b]		HF[a]	B3LYP[b]
8a[c]	−21.4	−22.7	**11a**	−19.4	−20.2
8b	−10.6	−7.5	**11b**	−4.6	−3.5
9a	−35.3	−34.3	**12a**	−33.9	−31.2
9b	−4.3	−5.1	**12b**	−2.8	−1.9
10a	−16.6	−19.3			
10b	−11.5	−8.6			

[a] HF/6-311+G(d,p) level of theory. [b] B3LYP/6-311+G(d,p) level. [c] The enthalpy of formation calculated at the MP2/6-311+G(d,p) level of theory for **8a**·ZnMe is −21.1 kcal/mol.

zinc compound through the formation of dative[31] bonds (eq 2).

$$\mathbf{A}\text{H} + \text{Me}_2\text{Zn} \rightarrow \mathbf{A}\cdot\text{ZnMe} + \text{CH}_4 \qquad (1)$$

$$\mathbf{B} + \text{Me}_2\text{Zn} \rightleftharpoons \mathbf{B}\cdot\text{ZnMe}_2 \qquad (2)$$

Monometallic Zinc Compounds. The reaction of a ligand containing an acidic hydrogen atom with dimethylzinc (Table 1 and Figure 3) is, not unexpectedly, a relatively exothermic process. For acidic ligands **A**H containing nitrogen and/or oxygen, $\Delta E \approx -20$ kcal/mol. If a Zn−S bond can be formed, the enthalpy of formation is considerably more negative ($\Delta E \approx -30$ kcal/mol). This is, as will be shown later, mainly due to a strong Zn−S hyperconjugative interaction. The favorable exothermicity of the reaction is responsible for the experimental finding that ligands such as β-amino alcohols and thiols react readily and nearly quantitatively with dialkylzinc compounds.

Ligands without an acidic hydrogen (**8b**−**12b**) are still capable of complexing with dimethylzinc to form energetically stable intermediates (eq 2 and Figure 4). The position of the equilibrium lies between −2 and −9 kcal/mol, as compared to the −20 or −30 kcal/mol calculated for the **A**-type ligands at the B3LYP level of theory (Table 1). The best **B**-type ligand is TMEDA (ligand **10b**; $\Delta E = -8.6$ kcal/mol) closely followed by the β-amino ether **8b**. The least stable **B**·ZnMe$_2$ complexes result when the ligand contains two oxygen atoms (**11b**) or two sulfur atoms (**12b**). In comparison to the **A**-type ligands, a fast equilibrium between free ligand, dialkylzinc compound, and the monomeric **B**·ZnMe$_2$ species can be expected for the **B** ligands.

For planning the synthesis of alkylzinc complexes containing bidentate chelate ligands, the following ranking established by these computational results should be helpful. Assuming that steric hindrance (bulky ligands) does not play an essential role, the stability of the expected **A**·ZnR or **B**·ZnR$_2$ species will decrease to the right as one varies the heteroatom combination in the ligand:

A-type ligands: NS > SS > NO > NN > OO

B-type ligands: NN > NO > NS > OO > SS

The HF and B3LYP calculations show that the two methods are satisfactorily consistent, yielding enthalpies of formation (ΔE_f) that lie within 3 kcal/mol of each other (Table 1). To provide an additional verification, ΔE_f for **8a**·ZnMe was calculated at the MP2/6-311+G(d,p) level of theory and is, with −21.1 kcal/mol, consistent with the HF (−21.4) and the B3LYP results (−22.7).

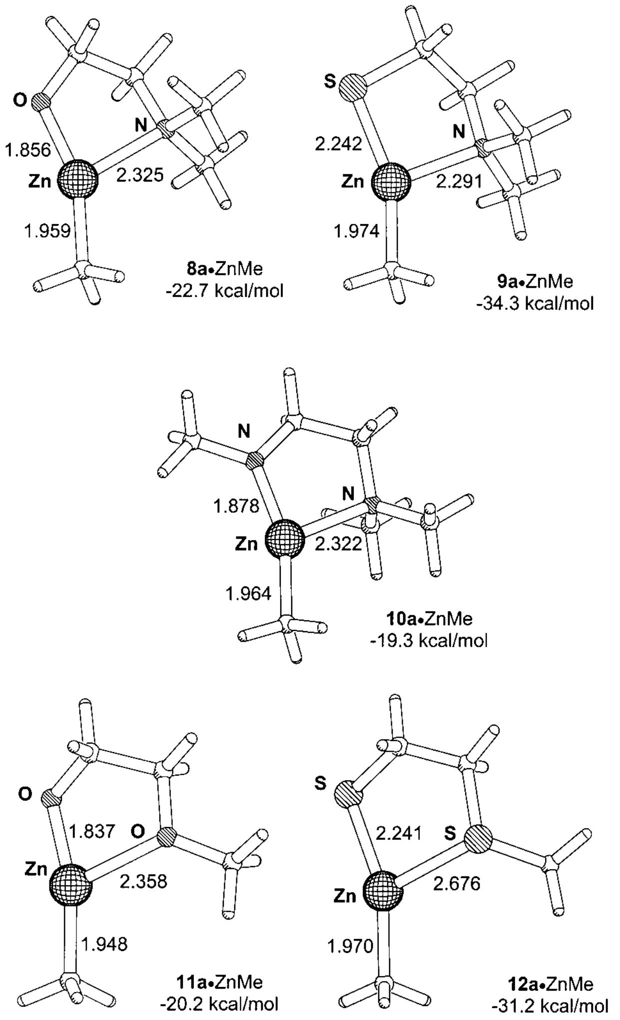

Figure 3. Structures of the zinc species generated by the reaction of ligands **8a**−**12a** with dimethylzinc, as calculated at the B3LYP/6-311+G(d,p) level of theory.

Calculations performed by Noyori et al. at the MP2/6-31G*//HF/3-21 level of theory for the reaction of 2-aminoethanol (ligand **8a**) with dimethylzinc have shown that a planar tricoordinate species (**8a**·ZnMe; see Figure 3) is formed that contains a covalent O−Zn and a dative[31] N−Zn bond.[10] The zinc atom is not fully sp^2-hybridized, since coordination of the nitrogen is rather weak. Variation of the ligand (**8a**−**12a**) in this contribution and a subsequent conformational search for monometallic species formed upon reaction with dimethylzinc at the much higher B3LYP/6-311+G(d,p) level of theory shows that the formation of a tricoordinate species with a planar structure at zinc (Figure 3) is a general characteristic for bidentate acidic (**A**-type) ligands.

A comparison of the structural parameters calculated for **8a**·ZnMe (Table 2) shows that the three methods yield similar structural parameters. (Experimental structural parameters for such compounds are not available, since existing X-ray structures[9,15,19] are dimers.) The MP2 method yields a Zn−N distance that is ca. 0.1

---

[31] Haaland, A. *Angew. Chem.* **1989**, *101*, 1017; *Angew. Chem., Int. Ed. Engl.* **1989**, *28*, 1011.

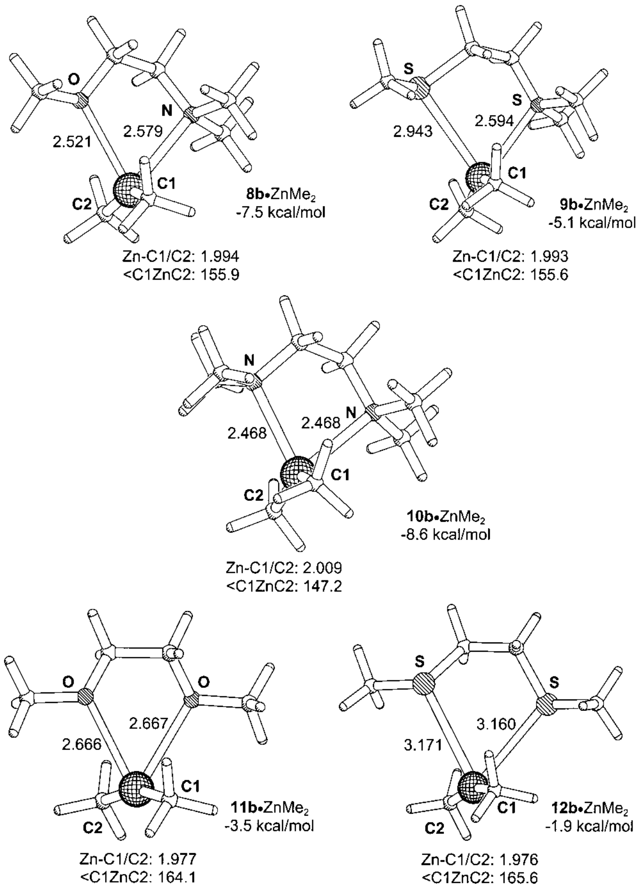

Figure 4. Structures of the zinc species generated by the reaction of ligands **8b**–**12b** with dimethylzinc, as calculated at the B3LYP/6-311+G(d,p) level of theory.

Table 2. Selected Structural Parameters (Å and deg) for 8a·ZnMe Calculated at Various Theoretical Levels[a]

	HF	B3LYP	MP2
Zn–N	2.316	2.325	2.224
Zn–O	1.854	1.856	1.843
Zn–C	1.997	1.959	1.934
∠NZnO	82.8	83.7	85.4
∠NZnC	120.1	118.8	117.9
∠OZnC	157.1	157.5	156.7

[a] The 6-311+G(d,p) basis set was employed throughout.

Å shorter than the HF and B3LYP results. Interestingly enough, increasing consideration of electron correlation effects (HF → B3LYP → MP2) causes the Zn–C bond to become increasingly and significantly shorter—an indication that a correlated method is necessary for the correct description of the Zn–C bonds in these complexes. Since it was not feasible to optimize all of the complexes considered here at the time-consuming MP2 level, Table 3 contains selected structural and electronic parameters for the monometallic species which were calculated at the B3LYP/6-311+G(d,p) level of theory.

The Zn–C bond in all five tricoordinate complexes **8a**·ZnMe–**12a**·ZnMe is highly polar. Exchanging a methyl group in dimethylzinc for a bidentate ligand increases the positive charge on zinc significantly. For example, $q_{Zn} = +1.40$ e in **8a**·ZnMe and +1.25 e in $ZnMe_2$. The charge on Zn is relatively constant at +1.40 e as the ligand is varied, with the only deviation occurring when a Zn–S bond is present. In this case, the charge on zinc is considerably lower (+1.28 e in **9a**·ZnMe and +1.23 e in **12a**·ZnMe) and parallels that found in free dimethylzinc. Although a rather large negative charge on the carbon atom is present, its charge distribution is relatively unaffected by the presence/absence of a ligand (−1.26 to −1.29 e) and can be directly compared to that calculated for dimethylzinc (−1.26 e). The ligand-induced polarization of the zinc center strengthens the Zn–C bond via a strong electrostatic contribution, which results in larger bond indexes (0.497–0.564) for the monometallic zinc complexes as compared to free $ZnMe_2$ (0.489). Exchanging a methyl group in $ZnMe_2$ for a bidentate **A**-type ligand thus *reduces* the capability of the monometallic zinc compound to act as a methyl anion transfer reagent.

As has been previously reported for **8a**·ZnMe,[10] the vacant s orbital on zinc, regardless of the identity of the **A**-type ligand, does not interact directly with the donor orbitals on the heteroatoms to form bonding orbitals. The NBO analyses performed here show that the predominant electronic interactions between the ligand and the zinc fragment are, of course, direct electrostatic interactions as well as three stabilizing hyperconjugative interactions (Table 3). The NBO procedure unambiguously assigns the Zn–X (X being the datively coordinated and Y being the deprotonated heteroatom) interactions to ionic-type bonds (Wiberg bond indices ≤0.10), whereas the Zn–Y interactions (bond indices $0.25 \geq \text{WBI} \leq 0.44$) can be viewed either as ionic bonds with a significant covalent portion or as weak covalent bonds that are significantly polarized in the direction of a $Zn^+–Y^-$ bond. The covalent contribution to the Zn–X bond is weakest when Y = N, O and strongest for Y = S.

The largest of the hyperconjugative interactions in the monometallic complexes **A**·ZnMe occurs between a lone pair in a p-type orbital on the deprotonated center Y and the antibonding σ^*_{Zn-C} orbital (Figure 5). This interaction is maximized when the heteroatom Y takes on a linear conformation with respect to the C–Zn bond. This $p \rightarrow \sigma^*_{Zn-C}$ interaction is responsible for the fact that the YZnC bond angle is much greater (158–165°) than would be expected (120°) for the trigonal planar geometry calculated for Zn. For Y = S (ligands **8b** and **12a**), an especially strong $p_S \rightarrow \sigma^*_{Zn-C}$ hyperconjugative interaction (ca. 30 kcal/mol larger than $p_N/p_O \rightarrow \sigma^*_{Zn-C}$ interactions) is present and is the reason for the increased stability of complexes containing an $Zn^+–S^-$ bond. The p-type lone pair orbital on Y also undergoes a smaller $p_Y \rightarrow s_{Zn}$ interaction with the empty s orbital on Zn. The third stabilizing hyperconjugative interaction between the ligand and the $Zn–CH_3$ fragment is a donation of electron density via a dative interaction between a lone pair in an sp^3-type orbital on the second heteroatom (X) and the σ^*_{Zn-C} orbital.

Complexation of type **B** ligands with dimethylzinc result in intermediates with an approximately tetrahedral zinc atom, with the largest bond angle being ∠CZnC (Figure 4 and Table 3). The ability of the ligand to complex with and polarize dimethylzinc can be directly estimated by the deviation of the ∠CZnC bond angle from 180°. The smaller the bond angle, the more stable the complex formed when the ligand reacts with dimethylzinc. Of the five ligands studied here, TMEDA

Table 3. Selected Structural and Electronic Properties for Monometallic A·ZnMe and B·$ZnMe_2$ Compounds Calculated at the B3LYP/6-311+G(d,p) Level of Theory

	8a·ZnMe	**8b**·ZnMe	**9a**·ZnMe	**9b**·ZnMe	**10a**·ZnMe	**10b**·ZnMe	**11a**·ZnMe	**11b**·ZnMe	**12a**·ZnMe	**12b**·ZnMe
Structural Parameters[a]										
X−Zn[b]	2.325	2.521	2.291	2.594	2.322	2.468	2.358	2.667	2.676	3.160
Y−Zn[c]	1.856	2.579	2.242	2.943	1.878	2.468	1.837	2.666	2.241	3.171
Zn−C[d]	1.959	1.994	1.974	1.993	1.964	2.009	1.948	1.977	1.970	1.976
∠YZnC	157.4	101.5	157.3	100.8	157.2	103.2	165.5	96.1	157.8	96.1
∠XZnC	118.9	98.6	113.2	98.9	117.6	102.4	114.4	98.8	112.4	96.2
∠CZnC		155.9		155.6		147.2		164.1		165.6
Wiberg Bond Indices[e]										
Y−Zn	0.076	0.043	0.075	0.050	0.051	0.050	0.045	0.020	0.107	0.015
X−Zn	0.258	0.005	0.432	0.039	0.261	0.050	0.274	0.020	0.441	0.016
Zn−C	0.545	0.464	0.497	0.431	0.534	0.409	0.564	0.455	0.504	0.468
NPA Charges[f,g]										
q_X	−0.636	−0.605	−0.642	−0.603	−0.641	−0.642	−0.654	−0.615	+0.101	+0.131
q_Y	−1.007	−0.618	−0.537	+0.177	−0.823	−0.642	−1.006	−1.006	−0.546	+0.131
q_{Zn}	+1.404	+1.337	+1.283	+1.316	+1.401	+1.364	+1.403	+1.311	+1.234	+1.238
q_C	−1.257	−1.283	−1.268	−1.282	−1.262	−1.294	−1.251	−1.275	−1.261	−1.270
Hybridization on Zn										
% s	96.1	96.3	96.7	96.2	96.6	96.6	95.6	96.0	96.4	95.6
% p	1.3	1.5	1.5	1.5	1.7	1.6	1.3	2.7	0.4	1.2
Hyperconjugative Interactions[h]										
	2.6	2.2	1.8	2.3	1.7	1.8	3.1	1.3	3.2	3.2
$sp^3_X \rightarrow s^*_{Zn-C}$	13.3	8.2	14.5	7.2	15.2	9.6	4.1	2.0	18.4	2.9
$p_Y/sp^3_Y \rightarrow s_{Zn-C}$	10.1		10.6		10.4		10.5		8.2	
$p_Y \rightarrow s^*_{Zn-C}$	54.8	2.9	83.6	8.3	76.2	9.6	57.7	2.0	86.4	2.9
$n_C \rightarrow s^*_{Zn-C}$		98.9		98.2		90.0		107.6		116.1

[a] Distances in angstroms and angles in degrees. [b] Dative bond (X:→ Zn). [c] "Covalent" bond (Y^-Zn^+). [d] The Zn−C bond length in dimethylzinc is 1.957 Å. [e] The Wiberg bond index for the Zn−C bond in dimethylzinc is 0.489 Å. [f] Charges in electrons. [g] The charge distributions calculated for free dimethylzinc at the B3LYP/6-311+G(d,p) level of theory are $q_C = -1.265$ and $q_{Zn} = +1.247$. [h] Values in kcal/mol.

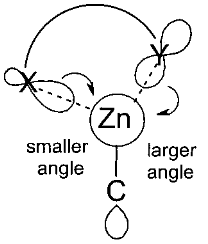

Figure 5. Orbital interactions between the bidentate ligand and the zinc fragment in **A**·ZnMe complexes (X, Y = N, O, S).

(**10b**) forms the most stable dimethylzinc adduct, closely followed by the β-amino ether (**8b**). The worst ligands are the ether (**11b**) and the thioether (**12b**).

NBO analyses of these complexes assign the dative Zn−X interactions to ionic bonds (Wiberg bond indices ≤0.05). Analogous to the tricoordinate **8a**·ZnMe−**12a**·ZnMe species, the empty s orbital on zinc does not undergo bond formation with any of the occupied lone pair orbitals on the heteroatoms of the ligand. As has been reported for dimethyl- and diphenylzinc,[18] the Zn−C bonds, regardless of the ligand type considered, have a nearly pure s character at Zn with very little contribution from the d orbitals. In addition, the NBO analysis indicates that the d orbitals on zinc do not participate in significant nonbonding or hyperconjugative interactions with donor orbitals originating from the ligand. In addition to the strong electrostatic interactions present, only two weak hyperconjugative interactions, one per heteroatom, are present, each of which being a donation of electron density from a sp^3 lone pair orbital on the heteroatom to one of the σ^*_{Zn-C} orbitals (Table 3).

Table 4. Enthalpies of Formation (kcal/mol) for the Generation of the Bimetallic Species A·Zn_2Me_3 Calculated Using the 6-311+G(d,p) Basis Set

ligand	HF	B3LYP	ligand	HF	B3LYP
8a	−12.7	−8.3	**11a**	−5.2	−2.4
9a	−3.6	−3.0	**12a**	−3.6	−2.7
10a	−12.5	−8.2			

Bimetallic Zinc Compounds. Monometallic zinc compounds formed from type **A** ligands (**A**·ZnMe) readily add an additional dimethylzinc to form energetically stable bimetallic **A**·Zn_2Me_3 complexes (Table 4 and Figure 6). The enthalpy of formation of the bimetallic species is exothermic by ca. 8 kcal/mol for all ligands that contain a Zn^+O^- bonding interaction (**8a** and **11a**). If a Zn^+S^- or a Zn^+N^- bond is present (**9a**, **10a**, and **12a**), the equilibrium position for the formation of the bimetallic complex is with ca. −3 kcal/mol somewhat less favorable. In each case the most basic heteroatom present (Y, the deprotonated one) accepts the dimethylzinc (Figure 6). Structures in which the dimethylzinc is located on the heteroatom X that is datively bonded to the zinc are not stationary points at either the HF or the B3LYP level of theory.

Interestingly enough, stationary points for bimetallic complexes containing **B**-type ligands could be found only on the HF level of theory and only for ligands **8b** and **9b**. Inclusion of electron correlation effects via the B3LYP method and reoptimization of these two complexes resulted in the formation of the monometallic **B**·ZnMe species and free dimethylzinc. Independent of the method employed, no stationary point for a bimetallic complex of the other three ligands (**10b**−**12b**) could be located.

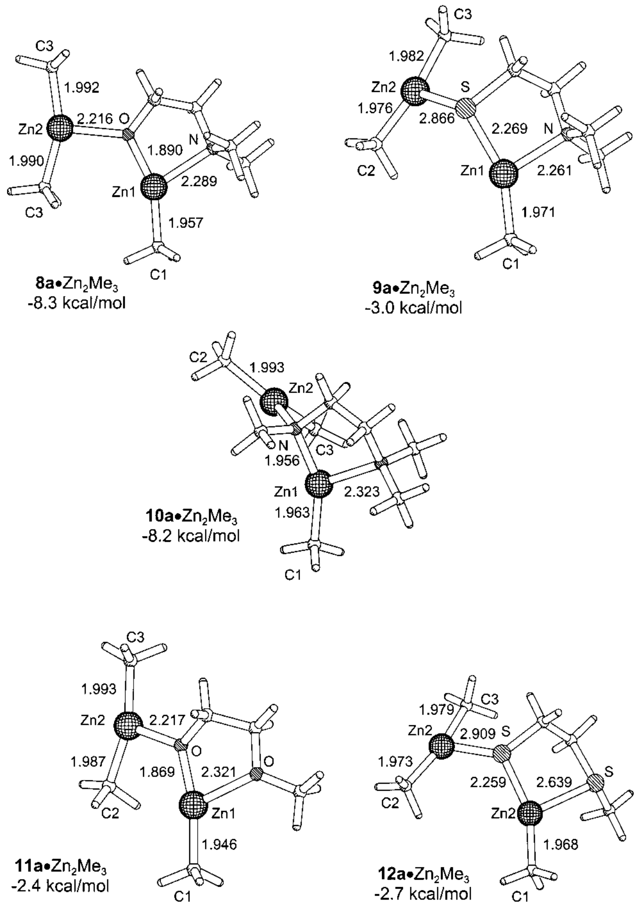

Figure 6. Structures of the bimetallic zinc species **A**·Zn$_2$Me$_3$ formed when ligands **8a**−**12a** react with dimethylzinc, as calculated at the B3LYP/6-311+G(d,p) level of theory.

Coordination of dimethylzinc to the **A**·ZnMe species does not cause a fundamental change in either the electronic interactions present in or the tricoordinate structure of the monometallic subunit (Figure 6 and Table 5). The second zinc atom Zn(2) also possesses a planar tricoordinate geometry. The Y−Zn(2) bond formed is longer (0.03−0.06 Å) than the Y−Zn(1) bond and is almost completely ionic in character with Wiberg bond indices of only 0.05−0.08. The predominate electronic interaction between the ligand and the Zn(2)Me$_2$ fragment is a weak hyperconjugative interaction between an sp-hybridized lone electron pair on Y and the antibonding $\sigma^*_{\mathrm{Zn(2)-C}}$ orbital. Zn(2)Me$_2$ is polarized upon complexation with the monometallic **A**·ZnMe subunit, which causes the ∠C(2)Zn(2)C(3) bond angle to become 20−30° smaller than 180°. At the same time, the Zn(2)−C(2)/C(3) bond orders are somewhat reduced as compared to both free dimethylzinc and to the Z(1)−C(1) bond present in the monometallic subunit. The negative charge on C(2)/C(3) is slightly increased, which indicates that the nucleophilicity of the methyl groups on Zn(2) is *enhanced* upon complexation with the **A**·ZnMe. As explicitly calculated at a lower level of theory in the case of ligand **8a** by Noyori et al.[10] and supported by the calculations presented here, methyl transfer to a carbonyl compound will occur out of the Zn(2)Me$_2$ unit. The methyl group bound to Zn(1) will not be transferred.

Table 5. Selected Structural and Electronic Properties for the Bimetallic A·Zn$_2$Me$_3$ Zinc Complexes Calculated at the B3LYP/6-311+G(d,p) Level of Theory

	8a· Zn$_2$Me$_3$	**9a**· Zn$_2$Me$_3$	**10a**· Zn$_2$Me$_3$	**11a**· Zn$_2$Me$_3$	**12a**· Zn$_2$Me$_3$
Structural Parameters[a]					
X−Zn(1)	2.289	2.269	2.323	2.321	2.639
Y−Zn(1)	1.890	2.261	1.956	1.869	2.259
Y−Zn(2)	2.216	2.866	2.268	2.217	2.909
Zn(1)−Zn(2)	3.587	4.277	3.247	3.522	4.364
Z(1)−C(1)	1.957	1.971	1.963	1.946	1.968
Zn(2)−C(2)	1.990	1.976	1.993	1.987	1.973
Zn(2)−C(3)	1.992	1.982	2.013	1.993	1.979
∠XZn(1)C(1)	119.0	115.3	115.2	113.5	114.3
∠YZn(1)C(1)	157.5	155.6	158.8	167.1	156.2
∠YZn(1)C(3)	103.1	98.8	102.2	103.6	98.3
∠C2Zn(2)C(3)	157.2	163.2	150.3	158.3	164.6
Wiberg Bond Order[b]					
X−Zn(1)	0.084	0.080	0.074	0.049	0.118
Y−Zn(1)	0.196	0.381	0.253	0.211	0.389
Y−Zn(2)	0.047	0.052	0.076	0.057	0.045
Zn(1)−Zn(2)	0.002	0.001	0.003	0.002	0.001
Zn(1)−C(1)	0.570	0.514	0.538	0.586	0.512
Zn(2)−C(2)	0.432	0.447	0.404	0.430	0.451
Zn(2)−C(3)	0.440	0.465	0.443	0.447	0.469
NPA Charges[c]					
q_{X}	−0.640	−0.645	−0.638	−0.658	+0.152
q_{Y}	−1.076	−0.564	−1.061	−1.074	−0.562
$q_{\mathrm{Zn(1)}}$	+1.420	+1.303	+1.386	+1.423	+1.252
$q_{\mathrm{Zn(2)}}$	+1.358	+1.295	+1.354	+1.354	+1.291
$q_{\mathrm{C(1)}}$	−1.247	−1.264	−1.254	−1.240	−1.256
$q_{\mathrm{C(2)}}$	−1.284	−1.270	−1.282	−1.286	−1.272
$q_{\mathrm{C(3)}}$	−1.292	−1.275	−1.303	−1.295	−1.267
Hyperconjugative Interactions[d]					
$sp^3(X) \rightarrow \sigma^*_{\mathrm{Zn(1)-C(1)}}$	14.6	15.8	13.4	5.4	20.4
$p(Y)^e \rightarrow s_{\mathrm{Zn(1)}}$	8.7	7.5	8.2	8.9	7.6
$p(Y) \rightarrow \sigma^*_{\mathrm{Zn(1)-C(1)}}$	43.5	75.1	53.5	47.6	77.3
$sp(Y)^e \rightarrow \sigma^*_{\mathrm{Zn(2)-C(2)}}$	10.6	8.5	17.7	10.6	6.9
$n(C_3) \rightarrow \sigma^*_{\mathrm{Zn(2)-C(2)}}$	100.2	107.4	92.1	100.4	108.6

[a] The sum of bond angles on both zinc atoms is 360°; the Zn−C bond length in free ZnMe$_2$ is 1.957 Å. [b] The Wiberg bond index for the Zn−C bond in ZnMe$_2$ is 0.489. [c] In electrons. The charge distributions calculated for free ZnMe$_2$ are $q_{\mathrm{C}} = -1.265$ and $q_{\mathrm{Zn}} = +1.247$. [d] In kcal/mol. [e] The lone pair orbital is approximately sp-hybridized.

The Lewis base coordination of Zn(2)Me$_2$ causes, independent of the identity of the ligand, a 0.02 e increase in the positive charge on the first zinc atom Zn(1) which, in turn, increases its Lewis acidity. The presence of the second zinc atom Zn(2) thus increases the capability of the first zinc atom Zn(1) to complex with a carbonyl compound. The increased positive charge on Zn(1) is accompanied by an increased polarization (increased negative charge) on C(1) and a slight increase in the Zn(1)−C(1) bond order as compared to the **A**·ZnMe monometallic complexes, thus making a C(1) methyl transfer even more unlikely.

The NBO analyses provide no indication for a bonding Zn−Zn interaction. For ligands containing a Zn$^+$O$^-$ or a Zn$^+$N$^-$ bonding interaction (**8a**, **10a**, and **11a**), the distance between the two metal centers is ca. 3.3−3.6 Å, which is directly comparable to the 3.4−3.6 Å distance reported for naturally occurring hydrolytic homobinuclear zinc enzymes such as leucine aminopeptidase,[32] phospholipase C,[33] or zinc metallo-β-lacta-

---

(32) Sträter, N.; Sherratt, D. J.; Colloms, S. D. *EMBO J.* **1999**, *16*, 4513. Sträter, N.; Lipscomb, W. N. *Biochemistry* **1995**, *34*, 9200.

(33) Uhlenbrock, S.; Krebs, B. *Angew. Chem.* **1992**, *104*, 1631; *Angew. Chem., Int. Ed. Engl.* **1992**, *31*, 1647. Hough, E.; Hansen, L. K.; Birknes, B.; Jynge, K.; Hansen, S.; Hordvik, A.; Little, C.; Dodson, E.; Derewenda, Z. *Nature* **1989**, *338*, 357.

mase.[34] If a Zn^+S^- bond is present (**9a** or **12a**), the Zn–Zn distance is increased to ca. 4.4 Å due to the sp^3 hybridization on sulfur.

Close inspection of the literature shows that catalytic systems containing OO chelate ligands usually contain OH functionalities in the ligand that are deprotonated upon reaction with dialkylzinc compounds.[17] For the few cases where a diamine has been reported to successfully catalyze the reaction of a dialkylzinc compound with an aldehyde, the diamine is generally of type **A** and not of type **B**.[16] An exception to this is TMEDA (ligand **10b**), which is reported to catalyze the addition of diethylzinc to benzaldehyde in 10% yield.[2] In addition, a recent study on this reaction employed several different fenchone-based ligands containing different coordination groups (an NO ligand of type **A** as well as a OO ligand and two NN ligands of type **B** were used).[35] All four ligands catalyzed the addition. Interestingly enough, the NO ligand (type **A**) resulted in an product with *R* configuration, whereas the three **B** ligands yielded the *S* enantiomer. QM/MM ONIOM calculations attribute this to repulsive interactions between alkyl groups at the zinc centers and the ligand.[35] Although **A**-type ligands are generally more effective, it is evident that the addition can take place when certain **B** ligands are employed.

Conclusions

Ligands containing two heteroatoms need to possess an acidic hydrogen (type **A** ligands) in order to efficiently form a monometallic **A**·ZnMe species upon reaction with a dialkylzinc compound. When the ligand cannot be deprotonated (type **B** ligands), a **B**·$ZnMe_2$ chelate complex is formed that is in equilibrium with the free ligand and dialkylzinc compound. Only monometallic **A**·ZnMe complexes formed from **A**-type ligands are capable of complexing with a second equivalent of dimethylzinc to form a **A**·Zn_2Me_3 bimetallic species. In the case of **B**-type ligands, the necessary bimetallic catalyst **14** cannot be generated via pathway **13** → **14** in Figure 7. Several possibilities for the **B**-ligand-mediated addition of organozinc compounds to carbonyls are feasible. (1) The addition could occur out of the monometallic complex (pathway **13** → **15** → **17** → products). (2) The carbonyl compound first adds to the monometallic compound **13**. The mixed species formed (**15**) then adds a second molecule of dialkylzinc (pathway **13** → **15** → **16** → products). (3) A slow alkyl transfer out of complex **15** followed by loss of an initial alcoholate molecule could result in a bimetallic species **18**, which then functions as the actual catalyst. All of these possibilities are currently being computationally investigated.

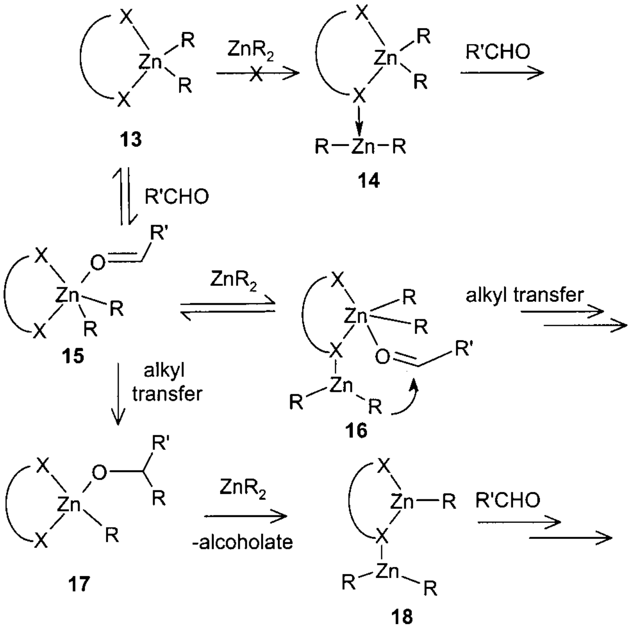

Figure 7. Mechanistic possibilities for the **B**-type ligand catalyzed addition of dialkylzincs to carbonyl compounds (X = N, O, S).

Acknowledgment. Financial support by the Deutsche Forschungsgemeinschaft (Sonderforschungsbereich 436, Jena, Germany) and by the Institut für Organische und Makromolekulare Chemie der Friedrich-Schiller-Universität, Jena, Germany, is gratefully acknowledged. A considerable amount of CPU time which led to the successful completion of this project was donated by the Hewlett-Packard Co. Special thanks goes to Prof. Dr. E. Anders (Jena, Germany) and his research group for stimulating discussions and valuable collaborations in the field of organozinc chemistry.

OM000783X

---

(34) Díaz, N.; Suárez, D.; Merz, K. M., Jr. *J. Am. Chem. Soc.* **2000**, *122*, 4197 and literature contained therein.

(35) Goldfuss, B.; Steigelmann, M.; Kahn, S. I.; Houk, K. N. *J. Org. Chem.* **2000**, *65*, 77.